Available online at www.sciencedirect.com
SCIENCE DIRECT
Thin Solid Films 513 (2006) 206–211
thin solid films
www.elsevier.com/locate/tsf

Surface modification of austenitic stainless steel on the surface of electric contact during low frequency current circulation

L. Nachez [a,*], B.J. Gómez [a], J. Ferrón [a], J. Feugeas [b]

[a] Instituto de Física Rosario (CONICET-UNR), Bvrd. 27 de Febrero 210 Bis., 2000 Rosario, Argentina
[b] Instituto de Desarrollo Tecnológico para la Industria Química (CONICET-UNL), Güemes 3450, 3000 Santa Fe, Argentina

Received 20 July 2005; received in revised form 30 November 2005; accepted 7 February 2006
Available online 24 March 2006

Abstract

During process of surface treatment of steels using plasmas (ion nitriding, physical vapor deposition and chemical vapor deposition, plasma immersion ion implantation, etc.), normally, one of the surfaces of the pieces has to be in electrical contact with one of the electrodes. In this work, we investigate the surface modification of the SAE EV12 stainless steel after being in electrical contact with the cathode during a normal process of ion nitriding. The physical conditions used were of a square wave electrical current of 10, 100 and 1000 Hz with an amplitude between 40 A m^{-2} and 80 A m^{-2} passing during 40 min. The treated surface was studied under Auger emission spectroscopy and grazing angle X-ray diffraction. The results have shown that a surface layer of 60 nm is strongly altered, and that the results depend on the frequency of the applied voltage and the pressure of contact between the surface and the cathode. In this surface layer, we could see the Fe–Cr, MnO and a carbide of the type $(Fe,Ni)_{23}C_6$ called haxonite, only reported in meteorites.

Keywords: Electromigration; Steel; Diffusion; Surface and interface states; Depth profiling

1. Introduction

It is known that a current circulation through the surface of steels produces modifications. This electric current surface modification is originated in the thermal effect caused by the Joule effect of the current. Normally, the current on the steel is induced by a high frequency alternating magnetic field induced by the also high frequency alternating external current. This heating happens on the surface of the material in a process that is known as skin effect. On the other hand, on magnetic steels, another heating effect can occur and it is originated in the hysteresis cycle loses due to the movements of the magnetic domains of the material. Nevertheless, this effect only occurs at temperatures below the Curie temperature of the material, which on steels depend on the carbon content. But this steel modification originated in electric currents and magnetic flux at the end originated in a heating process [1].

During the surface treatment of steels with plasmas, like chemical vapor deposition (CVD) and physical vapor deposition (PVD), plasma immersion ion implantation (PIII), ion nitriding, etc. [2,3], the samples to be treated have to be electrically connected to ground potential [4,5]. Normally (like in the ion nitriding, which is the particular case of this work) [6,7], the samples are electrically connected by gravity through one of the surfaces. This surface can suffer the effect of the pass of the current during an amount of time that can vary between tens of minutes to several hours, with an increase of the temperature up to 400 °C–600 °C. Depending on the system, the applied voltage can be, always thinking in the ion nitriding process, between 350 V and 700 V, DC or square wave modulated voltage with frequencies between 10 Hz and several hundreds kHz, with the active/passive ratio variable. The resulting current that circulates, and that will depend on the process and the electric parameters of the external circuit, results between 30 and 100 A m^{-2} [8]. On the other hand, in industrial applications, the piece to be treated sometimes has to be ion nitrided in all of his faces, implying that even

* Corresponding author.
E-mail address: nachez@ifir.edu.ar (L. Nachez).

0040-6090/$ - see front matter © 2006 Elsevier B.V. All rights reserved.
doi:10.1016/j.tsf.2006.02.012

the face used for electrical contact has to be ion nitrided. It means that, once the process is finished, the piece has to be turned to allow the ion nitriding of the former contact surface. Any change in the surface during the process originated by the pass of the electrical current through the surface can be a different starting point and a possible final state, different to the others surfaces of the piece.

In this work, we study the modification of a surface that is in contact with other (in our case, the cathode), due to the circulation of an electric current through them.

2. Experimental details

The work was done using samples specially prepared of SAE EV12 stainless steel with a composition (wt.%) of: C: 0.50/0.60, Mn: 7.00/10.00, P(max): 0.050, S(max): 0.030, Si(max): 0.25, Cr: 19.25/21.50, Ni: 1.50/2.75, N: 0.20/0.40. Samples were cut from a rod to a final size of 30 mm of diameter and 4 mm thick. The plane surfaces were polished with paper sand up to 3 μm, to be tested as surfaces of contact.

The experiments were done using an ion nitriding reactor [8] used in processes of surface treatment of steels. A schematic diagram of the reactor is shown in Fig. 1. The reactor consists of a 8×10^{-3} m^3 vacuum chamber of AISI 304 stainless steel connected to ground potential. Inside of the chamber, there is an electrode, also made of AISI 304 steel, connected to a power supply that can generate a square wave voltage, with amplitude variable up to 700 V, frequency variable between 0 Hz (DC) and 1000 Hz, and on/off ratio in each cycle variable between 100%/0% and 10%/90%. The voltage applied to the electrode was negative in all cases (cathode). The temperature is measured with a type K thermocouple. This thermocouple is in contact with the surface of the cathode on which the samples are placed.

In this type of reactor, the samples to be nitrided are connected to the cathode. A vacuum of 0.133 Pa is made in the chamber prior to the filling with the gases. The chamber is then filled with a mixture of nitrogen and hydrogen in variable proportions, with a filling pressure of 533.3 Pa. When a voltage (between 380 V and 600 V) is applied, a glow discharge (abnormal glow regime) is generated originating a density of current that normally results between 30 and 80 A m^{-2}.

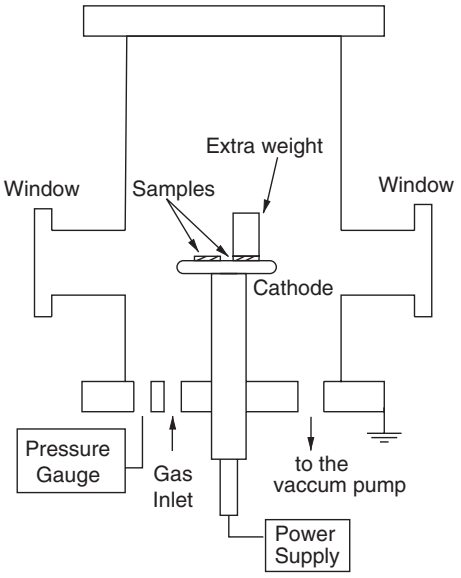

Fig. 1. Schematic diagram of the experimental configuration.

Table 1
Samples identification (S sample is the non-treated EV12)

Sample	Extra weight (kg)	Frequency of discharge (Hz)	Current density (A m^{-2})
S	–	–	–
S-1-U	0	10	59.4
S-2-U	0	100	47.1
S-3-U	0	1000	34.4
S-1-L	0.236	10	59.4
S-2-L	0.236	100	47.1
S-3-L	0.236	1000	34.4

Currently, the electric connection results from the simple contact between the surface of the sample and the surface of the stainless steel plate used as cathode. Then, the quality of the contact results from two factors: the roughness of both surfaces and the resulting pressure from the sample's weight.

Taking advantage of this facility, we derive our attention to the contact surface of the sample after a normal process of ion nitriding, monitoring the applied voltage (amplitude, frequency and on/off discharge ratio) and the discharge current.

On our experiments, we have worked with a constant temperature of 400 °C, with an on/off ratio of 40%/60% at three different frequencies: 10 Hz, 100 Hz and 1000 Hz. The applied voltage have been varied from 650 V for 10 Hz to 460 V for 1000 Hz and the external current varied from 1.041 A for 10 Hz to 0.815 A for 1000 Hz. These discharge conditions were used on two different samples with different cathode contact pressure. In one of them, the pressure was the result from the sample own weight and the other an extra 0.236 kg cylindrical weight was applied (Fig. 1). In all cases, the time of current circulation was of 40 min, counted after the system has reached thermal equilibrium. Temperature, current, voltage and flux are kept constant during each condition of treatment.

When the experiment was finished, the contact surface of the samples were studied using AES (Perkin Elmer-SAM 590A). After each spectrum, a thin layer of the sample was removed by sputtering with argon. In our case, the rate of sputtering was 8 Å/min.

Afterwards, diffractograms using GXRD technique were obtained. GXRD analyses were performed with a Phillips X' Pert diffractometer with K_α-Cu radiation (λ=1.54 Å). The angles of incidence used were 20°, 10°, 5° and 1°.

In Table 1, the different experimental situations are indicated.

3. Experimental results

The treated samples were studied by AES and GXRD. Metallography was also performed, but these analyses did not

show appreciable differences between the treated and the non-treated samples.

3.1. AES

AES allows to build a profile of the element compositionof the first nanometers of the surface layer. Using this method, we have made a profile of elements concentration down to an equivalent depth of 75 nm. We only show the profiles for samples S, S-2-U and S-2-L, since the other samples produced similar results. The results for S and S-2-L are shown in Figs. 2 and 3.

The results on the S sample (Fig. 2) show that, below the first 10 nm, the composition corresponds to the pure stainless steel used. The composition alteration on the first 10 nm can be related to the presence of oxygen that become combined with the elements constituent of the steel and is normally observed when stainless steels are analyzed through this method. C coming from atmosphere contamination is not shown in order to present the results in a more clear way, since it has no relevant information. Looking at the oxygen concentration profile, we can distinguish two regions: the first 3 nm, in which the oxygen concentration falls sharply from 60% in the surface to 5%, and a second region in which the concentration decreases continuously but less sharply, down to negligible values at a depth of 10 nm.

Looking at the AES depth of S-2-U (Fig. 3), we can see that the surface is depleted of Fe and Cr in comparison to the S sample. Presence of MnO can be observed in the first 50 nm. A high Mn concentration that reaches about a 45% at the surface (~5 nm) and then decreases to ~0% at 55 nm. The oxygen concentration profile follows the Mn concentration profile. The O concentration decreases to ~0% at 65 nm.

The study of the C concentration profile shows a concentration as high as 23% in the surface (contamination). The C concentration (not associated with contamination) has an

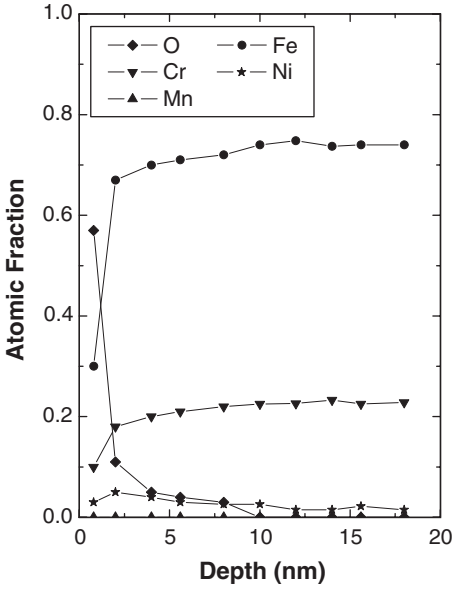

Fig. 2. AES profile for S sample.

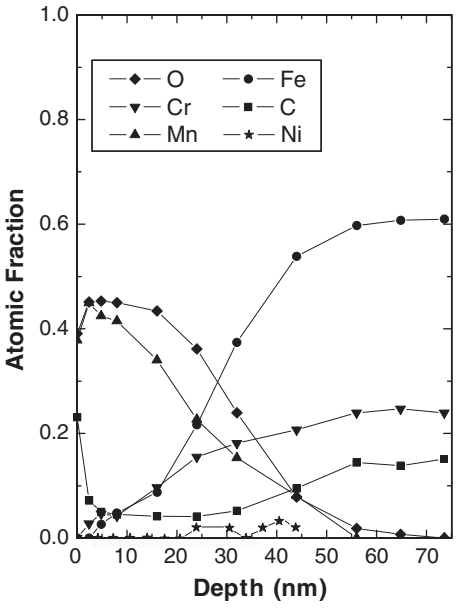

Fig. 3. AES profile for S-2-L sample.

almost constant value of ~6% between 5 and 30 nm. The concentration then increases and reaches the value of ~15% at 55 nm. There is no trace of N.

For sample S-2-L, the AES results do not differ (within the margin of error of the method) of those observed for sample S-2-U.

Looking at Fig. 4, the AES spectrograms of sample S-2-L shows at the surface the carbon peak (which is the temporal derivative of the peak intensity) is with an asymmetric profile. This shows that the carbon in the surface is pure (graphite) originated as a surface contamination in the atmosphere. At a depth of ≈ 20 nm, the spectrogram shows this peak strongly attenuated. Nevertheless, deeper, at 70 nm, the peak becomes intense again but now symmetric. This indicates that C is in form of a carbide; a fact that (as it will be shown later) is consistent with the GXRD results.

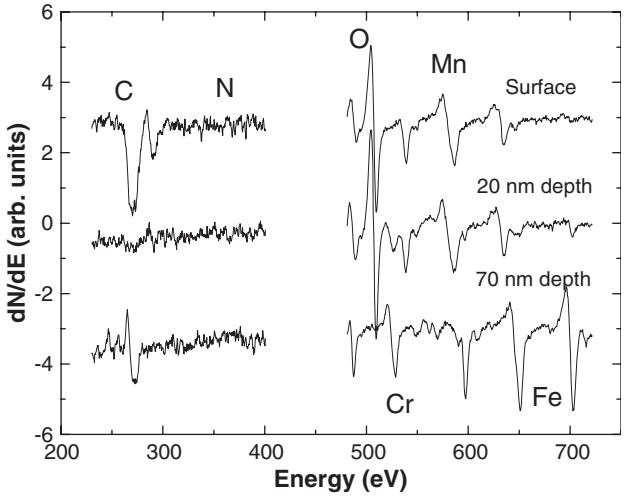

Fig. 4. AES spectrograms of sample S-2-L.

3.2. GXRD

The surfaces of all the samples used in this work were studied with the low angle incidence GXRD technique for 20°, 10°, 5° and 1°. We only show here the results for an angle of incidence of 10°. The results for 5° and 1° were similar to the ones obtained with 10°. We chose to present the diffractograms obtained with an angle of 10° over the diffractograms made with an angle of incidence of 20° because the intensity ratio of the studied peaks was better.

The intensities of all diffractograms are normalized to the $2\theta=43.42°$ austenite peak. The results for an angle of incidence of 10° are displayed in Figs. 5–7. Each figure corresponds to each of the frequencies (10 Hz, 100 Hz and 1000 Hz) of the applied voltage used, accompanied by the diffractogram corresponding to the S sample for comparative purposes. The analysis of S sample shows peaks at $2\theta=43.42°$, $2\theta=50.63°$, $2\theta=74.32°$, $2\theta=90.42°$ and $2\theta=95.16°$, corresponding to the crystal orientation planes (111), (200), (220), (311) and (222) of the austenite (γ-Fe).

The analysis of the surface in the case of applied voltage with a frequency of 10 Hz is shown in Fig. 5. In the diffractogram, sample S-1-U is possible to see; in addition to the peaks of austenite, others peak at $2\theta=44.59°$, $2\theta=64.84°$, $2\theta=82.26°$ and $2\theta=98.88°$, corresponding to the crystal orientation planes (110), (200), (211) and (220) of the phase (Fe–Cr), respectively. Also, other low intensity peaks at $2\theta=41.74°$, $2\theta=48.45°$, $2\theta=51.73°$ and $2\theta=76.96°$ (arrows in the figure) can be appreciated (these peaks were precisely identified later in the sample S-2-U with the aid of the appearance of a new peak).

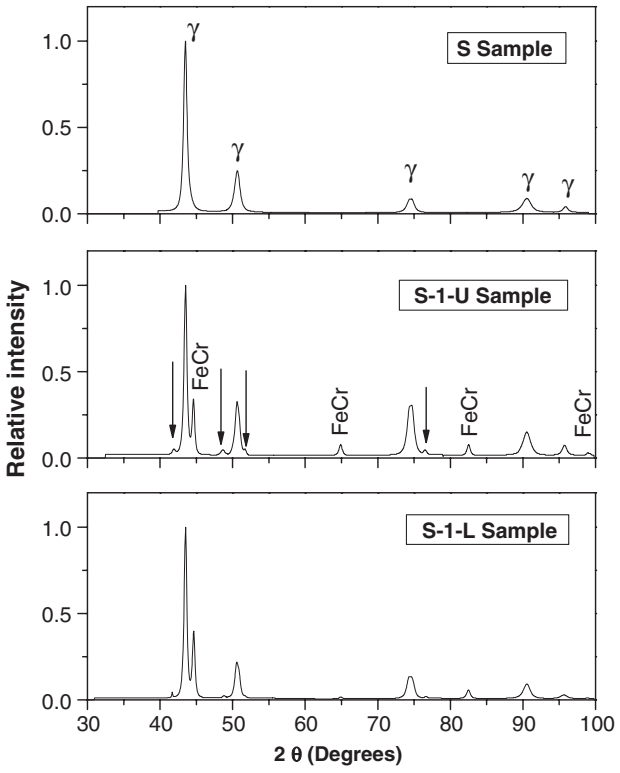

Fig. 5. GXRD diffractograms at 10 Hz for S, S-1-U and S-1-L samples.

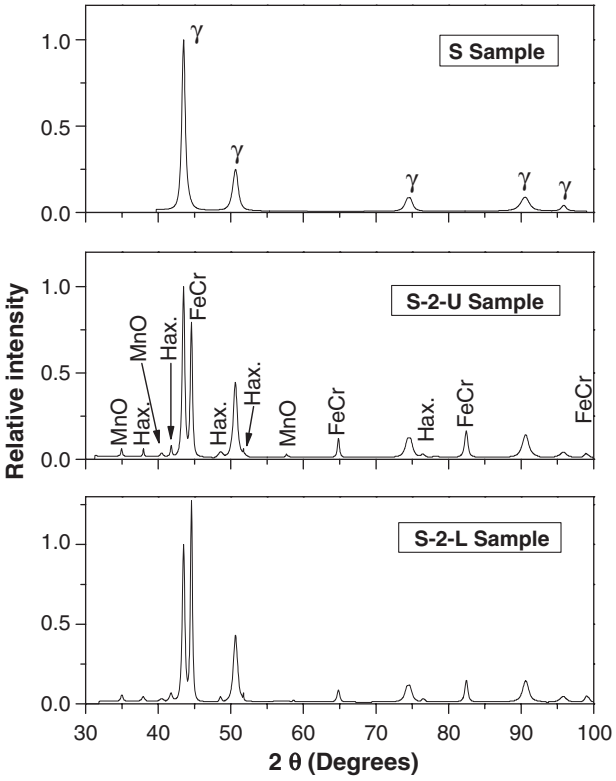

Fig. 6. GXRD diffractograms at 100 Hz for S, S-2-U and S-2-L samples.

The diffractogram corresponding to sample S-1-L presents the peaks of austenite, accompanied by the reflection peaks of (Fe–Cr) and the others at $2\theta=41.74°$, $2\theta=48.45°$, $2\theta=51.73°$ and

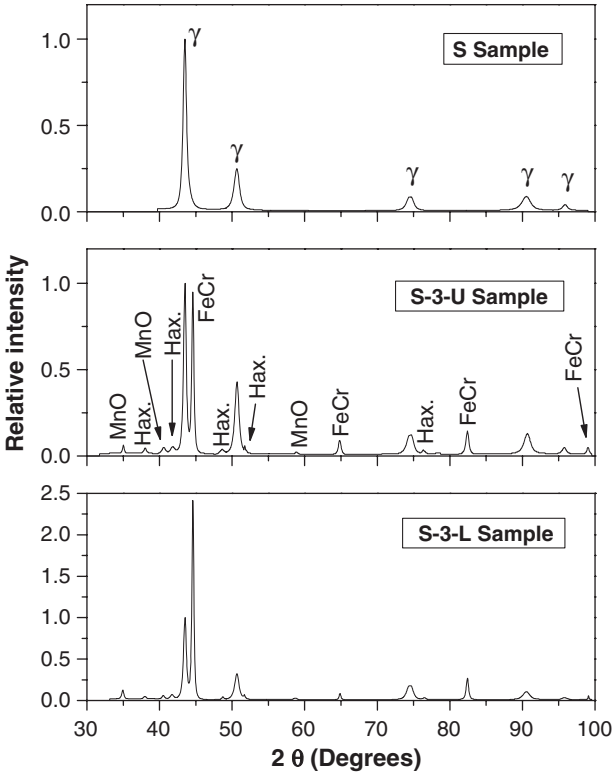

Fig. 7. GXRD diffractograms at 1000 Hz for S, S-3-U and S-3-L samples.

$2\theta = 76.96°$, but attenuated in intensity respect to the S-1-U. The analysis of the results corresponding to the voltage frequency of 100 Hz is shown in Fig. 6. For sample S-2-U, we can see that all the peaks observed for the austenitic phase and for the (Fe,Cr) phase already observed in the 10 Hz case (S-1-U sample) are present; with an important increase in the (Fe–Cr) peaks intensities. In addition, the peaks observed at $2\theta = 41.74°$, $2\theta = 48.45°$, $2\theta = 51.73°$ and $2\theta = 76.96°$ for the case of sample S-1-U are clearly present in this case, accompanied by four new peaks at $2\theta = 34.89°$, $2\theta = 37.95°$, $2\theta = 40.43°$ and $2\theta = 58.87°$. All those new peaks, except the one at $2\theta = 37.95°$, correspond to MnO.

Concentrating our attention on the non identified peaks observed at $2\theta = 37.95°$, $2\theta = 41.74°$, $2\theta = 48.45°$, $2\theta = 51.73°$ and $2\theta = 76.96°$, and considering all possible phases or compounds we reach the conclusion that it could correspond to the carbide type called "haxonite" (cubic structure, lattice parameter $a = 10.55$ Å) [9]. By observing the diffractograms corresponding to the S-2-L, we can see that it is basically similar to the S-2-U one, except that the peak at $2\theta = 44.59°$ (corresponding to the crystal plane orientation (110) of the (Fe–Cr)) results remarkably more intense. The analysis of the diffractograms for the case in which we use 1000 Hz as applied voltage frequency (S-3-U and S-3-L samples) shows the same set of diffraction peaks than the ones already observed for samples S-2-U and S-2-L. The diffractograms for this frequency are displayed on Fig. 7. For clarity purposes, we present in Fig. 8 an enlargement of the region with the most intense haxonite peaks (corresponding to Fig. 7). All those peaks were observed in all the tested samples.

A remarkable fact observed in the last three figures is the strong increase of the diffraction peak at $2\theta = 44.59°$ (corresponding to the (110) crystal orientation of (Fe–Cr)), with the increase of frequency. This can be analyzed by observing the results in Fig. 9, where we have plotted the intensity versus the contact pressure for the three frequencies used. We can observe that the $2\theta = 44.59°$ diffraction peak intensity increase with contact pressure and frequency of the applied voltage.

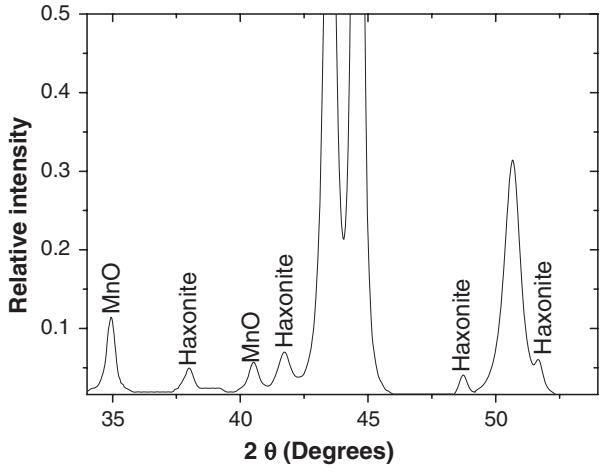

Fig. 8. Haxonite peaks.

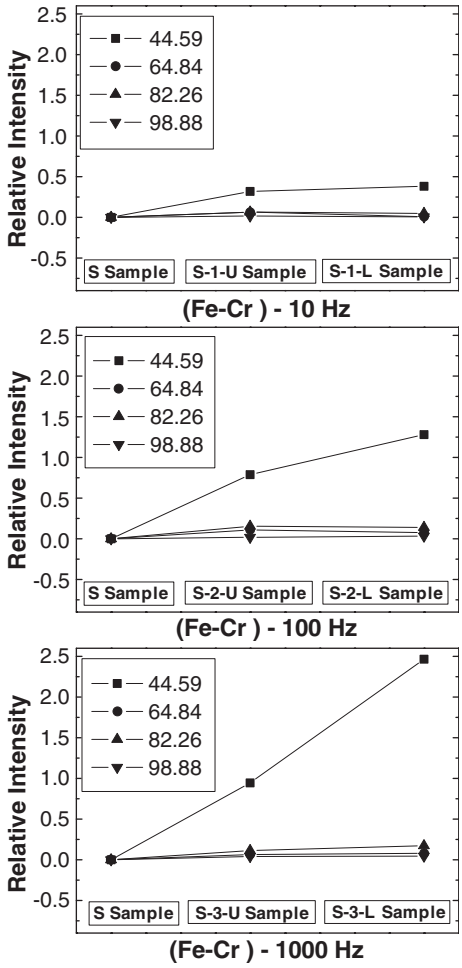

Fig. 9. Increase of the diffraction peak corresponding to the (110) crystal orientation of (Fe–Cr).

During the described process of ion nitriding, the samples reached the temperature of 400 °C. To explore the temperature effect without the simultaneous current passage, samples with similar characteristics to the ones used in the experiments described above were deposited on an AISI 304 stainless steel plane plate support. The lower surfaces of the samples were in contact with the surface of the support in the same way that occurs with the samples with the surface of the cathode during the ion nitriding process. The samples were introduced into an oven at the same filling pressure and mixture of gases used in the experiment, and heated at 400 °C during 40 min. The samples, removed after the heat treatment, were studied under GXRD. The resulting diffractograms show the typical structure corresponding to the base material, i.e. the ones shown for sample S in Figs. 4–6. These results show that the only effect of the temperature did not produce the observed changes on the surface during the ion nitriding process.

4. Discussion

We have studied the modification of the surface of contact of the SAE EV12 stainless steel during 40 min of current

circulation in the normal ion nitriding conditions. We could see that the surface suffers modifications that depend on the contact pressure and on the applied voltage frequency used. These modifications can be resumed as follows.

The AES concentration profile with depth analysis of the substrate has shown the element concentration corresponding to the normalized steel, except in the first nanometers in which atmospheric contamination was observed (normally present in AES analyses). The treated surfaces have shown important modifications consisting in a Mn concentration increasing in the surface layers, originated in a Mn migration from the bulk to the surface, as can be seen in the AES profiles. Fe and Cr concentrations are strongly reduced in the surface, being reestablished to their normal concentrations (corresponding to the substrate) at a depth of ≈60 nm.

The diffractograms of the surfaces of contact show in addition to the reflected peaks of austenite (reduced in intensity respect to the pure material) peaks corresponding to (Fe–Cr), MnO and others that can be attributed to the carbide "haxonite".

The MnO existence could be corroborated by the AES profiles. We could see that the concentration of both elements reaches the maximum at the surface being gradually and proportionally reduced down to the depth of ≈60 nm in which the Mn reaches its normal concentration. The O instead, that always has a concentration a little over the Mn concentration, reaches zero at ≈65 nm. Based on the Mn and O behaviour, the thickness of the Mn oxide was estimated, giving an approximate value of 40 nm.

It is clear that the O as well as the C at the surface layer are being affected by the electric current circulation at the surface of contact. The O because becomes bounded to the Mn and C because passes from a non-bounded state (graphite) to a bounded state.

The (Fe–Cr) compound formation is apparently influenced by the contact pressure and the voltage frequency. This fact can be seen through the reflected (110) peak of the (Fe–Cr), whose intensity strongly increases with the contact pressure and voltage frequency.

The most relevant modification on the steel surface structure has been observed through the reflection peaks at $2\theta = 37.95°$, $2\theta = 41.74°$, $2\theta = 48.45°$, $2\theta = 51.73°$ and $2\theta = 76.96$. These reflected angles and the intensity ratios between them are in accordance with the carbide identified as "haxonite". This carbide, discovered in 1971, was only observed up to date in several meteorites like Canyon Diablo meteorite in Coconino County, Arizona, USA and the Toluca meteorite in Xiquipilco, Mexico [10]. This carbide has the chemical formula $(Fe,Ni)_{23}C_6$ with the element composition consisting in 81.82% of Fe, 12.90% of Ni and 5.28% of C [11].

Metallography analyses of the treated surface did not show differences with the untreated material, since the modifications affect only the first nanometers of the surface.

The analysis of the results of the surface heated in an oven did not show modifications compared to the base material.

5. Conclusions

The plane surface of ASTM EV12 stainless steel suffers important changes under the passage of square wave electric current between 4 to 8 mA cm^{-2} and frequencies between 10 and 1000 Hz, changes that were found to be dependent on the contact pressure. The modifications were found to take place down to a depth of 60 nm for 40 min of electric current passage. It consists in the development of MnO and (Fe–Cr) compounds whose concentration reaches the maximum in the surface, and gradually decreasing down at 60 nm depth. The GXRD analyses have shown also the development of a carbide that was only reported in several meteorites, identified as haxonite ($(Fe, Ni)_{23}C_6$). It is clear that the circulation of electricity through an inter-phase is a phenomenon to be taken into account in the structure and phases modifications in materials, like in this case, an austenitic steel. In our case, the electric current passage and the contact correspond to the normal situation in a piece of steel during their surface treatment in processes like ion nitriding, PVD and CVD (among others). When the treatment of a piece has to be done in all of their surfaces, the piece has to be treated in at least two steps, using as contact surface, two different ones. The 60 nm surface layer modification found in this work has to be considered when the surface to be treated has been previously used as contact. The compound development in ion nitriding and the adherence of coatings in PVD or CVD process can be affected for this modified layer, as oppose to the surfaces not previously used as electric contact. For a full characterization of the process, further research has to be done using different type of steels, different discharge conditions and different pressures of contact.

Acknowledgements

The research was performed with the Grant PICT No. 12-06038 of the Agencia Nacional de Promoción de la Investigación Científica y Tecnológica de la República Argentina. We thank to H. Merayo for his collaboration in the experiment preparation.

References

[1] P.A. Hassell, N.V. Ross, ASM Handbook, Heat Treating, vol. 4ASM International, 1995, p. 164, Ch. Induction Heat Treating of Steel.
[2] T. Bell, Surf. Eng. 6 (1990) 31.
[3] K.S. Fancey, A. Matthews, IEEE Trans. Plasma Sci. 18 (1990) 207.
[4] J. Feugeas, G. Sanchez, C.O. de Gonzalez, J. Hermida, G. Scordia, Radiat. Eff. Defects Solids 128 (1994) 267.
[5] M.P. Fewell, S.C. Haydon, J. Phys., D: Appl. Phys. 30 (1997) 1778.
[6] M.J. Balwin, S.C. Haydon, M.P. Fewell, Surf. Coat. Technol. 97 (1997) 97.
[7] M. Wautelet, J.P. Dauchot, M. Hecq, Eur. J. Phys. 17 (1996) 88.
[8] J.N. Feugeas, J.D. Hermida, B.J. Gómez, G. Kellermann, P.E. Craievich, J. Phys., D: Appl. Phys. 32 (1999) 2228.
[9] Pdf-2 Database, JCPDS-International Center for Diffraction Data, PA, USA, Sets 1-47, 1997, Card 25-0405.
[10] E.R.D. Scott, Nature 229 (1971) 61.
[11] E.R.D. Scott, R.W. Bild, Geochim. Cosmochim. Acta 38 (1974) 1379.